Interactive global change factors mitigate soil aggregation and carbon change in a semi-arid grassland

Running title: Interactive global change effects on soil C

Tongshuo Bai[1], Peng Wang[1], Steven J. Hall[2], Fuwei Wang[1], Chenglong Ye[1], Zhen Li[1], Shijie Li[1], Luyao Zhou[1], Yunpeng Qiu[1], Jiuxin Guo[1, 3], Hui Guo[1], Yi Wang[4]*, Shuijin Hu[1, 5]*

[1]Ecosystem Ecology Laboratory, College of Resources and Environmental Sciences, Nanjing Agricultural University, Nanjing 210095, China

[2]Department of Ecology, Evolution, and Organismal Biology, Iowa State University, Ames, IA 50011, USA

[3]International Magnesium Institute, College of Resources and Environment, Fujian Agriculture and Forestry University, Fuzhou, 350002, China

[4]State key Laboratory of Loess and Quaternary Geology, Institute of Earth Environment, Chinese Academy of Sciences, Xi'an 710061, China

[5]Department of Entomology & Plant Pathology, North Carolina State University, Raleigh, NC 27695, USA

***Correspondence:**

Shuijin Hu

Email: shuijin_hu@hotmail.com; Phone: +001 919-515-2097

Yi Wang

Email: wangyi@ieecas.cn; Phone: +86 29 62336290

This article has been accepted for publication and undergone full peer review but has not been through the copyediting, typesetting, pagination and proofreading process, which may lead to differences between this version and the Version of Record. Please cite this article as doi: 10.1111/GCB.15220

Abstract

The ongoing global change is multi-faceted, but the interactive effects of multiple drivers on persistence of soil carbon (C) are poorly understood. We examined the effects of warming, reactive nitrogen (N) inputs (12 g N m^{-2} y^{-1}) and altered precipitation (+ or – 30% ambient) on soil aggregates and mineral-associated C in a 4-yr manipulation experiment with a semi-arid grassland on China's Loess Plateau. Our results showed that in the absence of N inputs, precipitation additions significantly enhanced soil aggregation and promoted the coupling between aggregation and both soil fungal biomass and exchangeable Mg^{2+}. However, N inputs negated the promotional effects of increased precipitation, mainly through suppressing fungal growth and altering soil pH and clay-Mg^{2+}-OC bridging. Warming increased C content in the mineral-associated fraction, likely by increasing inputs of root-derived C, and reducing turnover of existing mineral-associated C due to suppression of fungal growth and soil respiration. Together, our results provide new insights into the potential mechanisms through which multiple global change factors control soil C persistence in arid and semi-arid grasslands. These findings suggest that the interactive effects among global change factors should be incorporated to predict the soil C dynamics under future global change scenarios.

Keywords: Global change, carbonate, aggregate stability, mineral-associated C, soil respiration, N-induced acidification

1. Introduction

Human activities such as fossil fuel combustion and fertilizer applications have induced the ongoing global change, leading to elevated air temperature, altered precipitation regimes, and atmospheric nitrogen (N) deposition (Dillon et al., 2010). These alterations can strongly influence plant photosynthesis, plant production, and microbial decomposition, modifying the carbon (C) cycling of the terrestrial biosphere and thus land–atmosphere CO_2 fluxes (Lu et al., 2011; Liu et al., 2016; Wang et al., 2019). Soil is the largest terrestrial reservoir of active C (Jobbagy & Jackson, 2000), containing more organic C than the C in vegetation and the atmospheric CO_2

combined (Lal, 2008). Isotopic and spectroscopic data indicate that a significant proportion of persistent soil organic matter (SOM) is derived from C with relatively labile organic compounds, such as saccharides and proteins (Schmidt et al., 2011). This suggests that spatial inaccessibility for microbes to organic C, rather than bond strength or molecular complexity, exert an important impact on the persistence of soil C (Dungait et al., 2012; Lehmann & Kleber, 2015). Soil aggregation and transformations of plant-originated C into slower-turnover C fractions, such as chemical adsorption of organic C by soil minerals, may facilitate long-term C stabilization (Six et al., 2004; Yu et al., 2017).

Global change drivers can influence soil aggregation and the mineral protection of soil C. For example, warming has been shown to reduce soil aggregate stability in an alpine meadow (Guan et al., 2018) but promote matrix-stabilized C by mineral association in a mountain grassland (Poeplau et al., 2017). Also, warming may shift the soil microbial community and promote decomposition of microbial secondary compounds that contribute to soil aggregate formation (Rillig et al., 2002; Lehmann et al., 2017). Similarly, changes in rainfall can alter soil C persistence. Campos et al. (2017) reported that rainfall increase promoted aggregate protection of soil C in an 18-yr experiment. In contrast, Berhe et al. (2012) showed that added precipitation markedly reduced Fe/Al oxide-associated C. Contrasting effects of reactive N inputs on soil aggregation have also been reported: they can promote (Wilson et al., 2009) or reduce soil aggregation (Shen et al., 2018), depending on their impact on fine roots and fungal biomass (Miller & Jastrow, 1990). Similarly, reactive N input may increase mineral-associated C through increasing N supplies to microbes and reducing microbial decomposition of old microbial residues (Griepentrog et al., 2014). Alternatively, it may reduce mineral-associated C by inducing soil acidification and dissolution of C-mineral complexes bonded by polyvalent cation bridges (Ye et al., 2018). Yet, it remains largely unknown how different global change factors (altered precipitation, temperature, and N inputs) may interactively affect soil chemistry and biological processes that control soil aggregation and mineral-associated organic C under field conditions.

The ongoing global change is multifaceted (IPCC, 2013) and interactions of multiple environmental change factors may enhance or offset the effects of individual factors on soil C

(Rillig et al., 2019). While some studies documented additive effects of multiple global change drivers on soil C storage (Yue et al., 2017; Dietzen et al., 2019), other results suggest that direct extrapolation of single factor effects to the multi-faceted reality based on the "additive effect" assumption may overestimate or underestimate the impacts on soil C fluxes (Zhou et al., 2016; Ni et al., 2017). For example, warming effects on soil CO_2 efflux were significantly dependent on water availability in a semi-arid Mongolian grassland (Zhou et al., 2012). Extreme rainfalls and snowfalls have also been shown to mediate the responses of soil respiration to N input in a rainfed maize-cultivated cropland (Chen et al., 2017). Thus, results from single factor experiment may poorly predict the interactive effects of multiple global change drivers under future global change scenarios. However, few studies have explicitly examined the effects of multiple global change factors on soil C persistence (i.e. soil aggregation and mineral protection of soil C), in particular in the arid and semi-arid ecosystems (Henry et al., 2005), where C dynamics are more sensitive to global changes than mesic ecosystems (Poulter et al., 2014, Ahlstrom et al., 2015).

China's Loess Plateau covers a huge area of arid and semi-arid ecosystems (total at 620 000 km^2, about 6.5% of the area of China) (Shi & Shao, 2000). The soil across the Plateau is largely alkaline Calcisol with a large potential of carbonate accumulation (Wu et al., 2009). Ecosystems in this region are often fragile and highly sensitive to global change. For example, N fertilizers can affect abiotic processes and lead to carbonate dissolution (Zamanian et al., 2018) and cation (i.e. Ca^{2+} and Mg^{2+}) release and losses (Chen et al., 2016). Also, circulation-driven variations in both precipitation and temperature in semi-arid ecosystems (Ahlstrom et al., 2015) critically affect biological processes, altering plant productivity in grasslands (Guo et al., 2017). Yet, the direction and magnitude of effects of interacting factors on soil C dynamics have not been explored.

We conducted a field experiment simulating multiple factors (warming, N inputs and altered precipitation) in a grassland on Loess Plateau to examine their effects on soil C persistence and explore the underlying mechanisms. Because of severe water limitation with potential high evapotranspiration in dryland ecosystems, a precipitation increase would likely alleviate water stress and promote plant and microbial growth. Thus, precipitation likely plays a major in regulating root-derived C input and root-mediated aggregate stability (Miller & Jastrow, 1990; Hu

et al., 1995). Given that alkaline soils are usually enriched with calcium (Ca) and magnesium (Mg), and cation-C association is an important mechanism mediating soil C persistence (Rowley et al., 2018, Ye et al., 2018), we proposed that precipitation increase would increase exchangeable Ca^{2+} and Mg^{2+} in soil solution and promote formation of Ca- and/or Mg-C complexes, as well as enhance fungal growth and fungal-mediated aggregation (Hypothesis 1). However, N inputs would suppress both fungal growth and aggregation, and N-induced acidification would disassociate Ca- and/or Mg-C complexes, offsetting the impact of precipitaiton increase (Hypothesis 2). Further, we predicted that warming would reduce SOC by increasing microbial enzymatic activities and turnover of labile and accessible organic C and offset the impact of precipitation increase on SOC (Hypothesis 3).

2. Materials and methods

2.1. Study site, experimental design, and soil sampling

The field experiment was located at the Yunwu Mountains Natural Preserve (106°21′–106°27′E, 36°10′–36°17′N) on the Loess Plateau, Guyuan, Ningxia Hui Autonomous Region, China. The area of this reserve is 4000 ha in size and has an elevation of 1800–2100 m. It is a loess covered area of low hills. Mean annual temperature is 7 °C, with the highest mean monthly temperature in July (22–25 °C) and the lowest in January (-14 °C). The climate is a temperate, arid and semi-arid continental monsoon with an average annual rainfall of 400–450 mm. With potential evaporation of 1330–1640 mm, the grassland is extremely water limited. The soil is a mountain gray-cinnamon type classified as a Calci-Orthic Aridisol, equivalent to a Haplic Calcisol in the FAO/UNESCO system. It has a bulk density of 1.1 g cm^{-3} and is with high infiltration capacity. The plant community is dominated by *Artemisia sacrorum* Ledeb., *Stipa przewalskyi* Roshev., *Stipa grandis* P. Smirn. and *Thymus mongolicus* Ronn.

With the aim to investigate effects of warming, reactive N inputs, altered precipitation, and their interactive effects on plant communities and soil processes, a multi-factorial field experiment was established on a largely flat hilltop in June 2015 (Figure 1a). The manipulative experiment had a randomized block design with three treatment factors and their combinations. It included

two warming levels [control (CK) and whole-year warming (W)], two N levels [control (CK) and 12 g N m^{-2} $year^{-1}$ N inputs], and three precipitation levels [30% precipitation reduction (Pr), control (CK), and 30% precipitation increase (Pi)], resulting in 12 treatments (2 N levels × 2 warming levels × 3 precipitation levels). Each treatment had four replicates, i.e. four blocks, leading to a total of 48 plots. Each plot was 4 × 4 m in size and 1.5 m away from other plots in each block. The distance between each block was 5 m. The open-top chamber (OTC) for the warming treatment had a hexagonal design made of transparent plexiglass, each with 1.19 m width at the top and 1.5 m at the bottom, and a height of 51.76 cm (Figure 1b). For the Pr treatment, multiple tilted v-shaped transparent plexiglass sheets were placed 1 m above the soil surface on a metal hanger over each plot (Figure 1c). The transparent plexiglass covered 30% of the soil surface area and the precipitation blocked by the v-shaped plexiglass was collected by plastic containers. The water collected in one plot was then manually added into the nearest plot that was designated for Pi treatment within 24–48 hours after the rainfall event ended. In this way, each Pi plot received an addition of 30% natural precipitation without changing the frequency of natural precipitation. Nitrogen was applied twice a year in early May and early July in the form of urea at a rate of 6 g N m^{-2} each time (total input of 12 g N m^{-2} y^{-1}). We applied N to simulate fertilization, because fertilization is very common in this region to increase yield of forage grass.

After four years of continuous field treatments, soil samples were collected at 0–10 cm depth in late August 2018. Three soil cores (5 cm diameter) were randomly taken from each plot and then thoroughly mixed to form a single sample. Soil samples were kept in a cooler with ice and shipped to the lab within 48 h. Visible roots were rinsed under running water, collected on a 1-mm screen, oven-dried at 65 °C, and weighed to calculate the root biomass. After visible roots and rocks were removed, fresh soil samples were then divided into two parts: one subsample was air dried and passed through a 5 mm sieve for physio-chemical analysis and the other subsample was passed through a 2 mm sieve and kept at 4 °C for microbial analyses.

2.2 Soil chemical and microbial analyses

Soil organic carbon (SOC) and total nitrogen (TN) were analyzed using a CN analyzer (Elementar

Vario Micro cube, Hanau, Germany). Soil carbonate was determined by measurement of CO_2 by gas chromatography following sample acidification (Amundson et al., 1988). Soil pH was measured in a 1:5 ratio of soil to CO_2-free water with a pH meter (Starter-3100, Ohaus, Newark, NJ, USA) with an Expert Pro-ISM-IP67 probe. Microbial biomass C (MBC) was determined using the chloroform fumigation extraction method (Vance et al., 1987). Briefly, 12.5 g fresh soil was fumigated with chloroform for 48 hours and extracted with 50 mL 0.5 M K_2SO_4. After being shaken for 30 minutes, the supernatant was filtered. Also, a non-fumigated soil was extracted directly and used as the control. Dissolved organic C in extracts was measured on a TOC analyzer (Elementar Vario TOC cube, Hanau, Germany) and the differences between the fumigated and non-fumigated samples were converted into microbial biomass C with a conversion factor of 0.38. Dissolved inorganic N (DIN, i.e. NO_3^--N and NH_4^+-N) in the extracts of non-fumigated soils was determined on a flow injection autoanalyzer (Skalar San++ CFA, Erkelenz, Germany). Soil exchangeable Ca^{2+} and Mg^{2+} were extracted with 1M ammonium acetate (Hendershot et al., 1993) and were determined with an inductive coupled plasma emission spectrophotometer Agilent 710 ICP-OES (Agilent Technologies, Palo Alto, CA, USA).

Composition of the soil microbial community was characterized by analyzing phospholipid fatty acids (PLFAs) (Bossio & Scow, 1998). Briefly, lipids were extracted from 5.0 g freeze-dried soil with a mixture of chloroform, methanol and citrate buffer (volume ratio: 1:2:0.8), and the phospholipids in the organic phase were separated using a solid-phase silica column (Agilent Technologies, Palo Alto, CA, USA). After mild alkaline methanolysis, the resulting fatty acid methyl esters were identified using an Agilent 6850 Gas Chromatograph. The dominant PLFAs were classified as Gram-positive bacteria (i14:0, i15:0, a15:0, i16:0, i17:0 and a17:0), Gram-negative bacteria (16:1ώ9c, cy17:0, 18:1ώ9c and cy19:0), saprotrophic fungi (18:2ώ6c), arbuscular mycorrhizal fungi (AMF) (16:1ώ5c),actinomycetes (10Me16:0, 10Me17:0, 10Me18:0), eukaryote (18:3ώ6c, 16:3ώ6c, 22:2ώ6c) and anaerobe (18:1ώ7c). We added up PLFA 18:2ώ6c and 16:1ώ5c to indicate fungal biomass and added up PLFAs of Gram-positive bacteria and Gram-negative bacteria to indicate bacteria biomass. The abundance of individual PLFAs was expressed as fatty acid nmol g^{-1} dry soil.

2.3 Aggregate and SOC fractionation

Soils were separated using the wet sieving and density fractionation approach modified from Tamura et al. (2017) and Guan et al. (2018). Briefly, 30.0 g air dried soil was spread on a 250 μm sieve and wetted with 500mL of deionized water for 10 minutes in 2 L beaker at room temperature, and the sieve was moved up and down 3 cm with 100 repetitions during a period of 10 min. The fraction remaining on the 250 μm sieve was washed into a petri dish. The remaining soil solution in the beaker was poured onto a 53 μm sieve and the sieving process was repeated. The remaining fraction in the beaker (<53 μm) and two larger fractions were then dried at 60 °C for 48 h. Three fractions, that is, >250 μm, 53–250 μm and <53 μm fractions were thus obtained.

In order to more accurately estimate the mass and C content of each size fraction, the free organic materials that were not held within aggregates or silt/clay were removed. Briefly, each fraction was gently poured into a 50 ml polycarbonate centrifuge tube that contained 40 mL sodium iodide (NaI) solution (at density of 1.8 g cm^{-3}). The tube was slightly shaken by hand for 5 times without any dispersion and allowed to settle down at room temperature for 2 h, and the light fraction was then obtained by centrifugation (1,500 g). After repeating the procedure three times, the floating free light materials (< 1.8 g cm^{-3}) were collected, washed with deionized water for 4 times to remove NaI, and kept separately. The heavy fraction (> 1.8 g cm^{-3}) was also washed with 40 mL deionized water and then centrifuged for 10 min at 1,500 g for 4 times to remove NaI. The remaining heavy fraction in each tube was dried at 60 °C for 48 h. Finally, we obtained four physical fractions for each field sample: free light organic materials (a composite fraction of all the light organic materials obtained from >250 μm, 53–250 μm and <53 μm fractions), and macroaggregate (>250 μm), microaggregate (53–250 μm), and silt-clay (<53 μm) heavy fractions. The macro- and micro- aggregates were composite fractions that contained occluded silt, clay and partly decomposed litter. We calculated weight and C concentrations in different aggregate-size fractions without sand-free correction (Castro-Filho et al., 2002; Shen et al., 2018). The C in the silt-clay fraction was considered as the mineral-associated C because the density fractionation described above removed all of the light fraction (Stewart et al., 2008). Subsamples of aggregate

size fractions (i.e., macroaggregates, microaggregates, and the silt-clay fraction) were treated with 1 M HCl for 24 h at room temperature to remove any inorganic C prior to determination of SOC and TN.

2.4 Soil respiration measurement

To measure soil respiration (Rs), in one subplot of each plot, a thin-walled polyvinyl chloride respiration collar (20 cm diameter and 5 cm height) was permanently inserted approximately 3 cm into the soil to minimize the potential mechanical disturbance during the experiment establishment in June 2015. We measured Rs using an IRGA infrared gas analyzer (Li-8100, LiCor, Lincoln, NE, USA) weekly during May–September in 2018, yielding 18 measurements for the study. While measuring soil respiration, we also measured soil temperature and moisture at the 10 cm depth as well as air temperature. At each sampling time, measurements were performed between 8:00 and 12:00 h. Each sampling campaign lasted 3–4 h, during which we measured four blocks in the same sequence to reduce temporal and spatial biases. In addition, we frequently clipped living plants inside the PVC collars and left the clipped plant materials on the soil within the collars (Wan et al., 2007). Each clipping was finished at least one day before the soil respiration measurement to minimize disturbance influence.

2.5 Calculations and statistical analyses

Aggregate stability was expressed as mean weight diameter (MWD), calculated as the sum of the mass fraction, multiplied by the inter-sieve size in accordance with the formula:

$$\mathrm{MWD} = \sum d * m$$

where *d* is the mean diameter of the two sieves (mm) and *m* is relative fraction mass of aggregates (%) (Castro-Filho et al., 2002).

We used linear mixed models to assess how soil variables were affected by treatments, with block as a random effect and treatments as fixed effects. For the measurements of soil respiration, soil temperature, soil moisture, and air temperature, similar models were used with block and plot introduced as random effects (mixed effects model; lmer function from the lme4 package). The

residuals from the models were examined for normality and homoscedasticity using graphical diagnostic plots (i.e. Q–Q plots and residuals plots) (Quinn & Keough, 2002). Logarithmic (log_{10}) transformations were applied when the assumptions were violated for root biomass and DIN content. To further interpret significant interactions, data were divided into subsets based on one of the factors of the interaction and *post hoc* comparisons were done for each level of the factor. The Tukey's HSD test was used for *post hoc* comparisons of factors with more than two levels (glht function from the multcomp package). Linear regressions were conducted to analyze the response of soil carbonate to exchangeable Mg^{2+} and responses of exchangeable Ca^{2+}, Mg^{2+} and fungal biomass to MWD with block as a random effect.

3. Results

3.1 Air temperature, soil temperature and soil moisture

The average air temperature during the growing season was 22.5 °C and warming by OTCs significantly increased it by 1.4 ± 0.2 °C ($P < 0.0001$, Table S1, Figure S1). Warming had no effect on soil temperature at 10 cm depth ($P = 0.8629$), but significantly decreased soil moisture by 15.5 ± 1.7% during the growing season ($P < 0.0001$). Altered precipitation significantly affected soil moisture, with a 3.5 ± 2.1% decrease in the Pr treatment and with a 6.8 ± 1.8% increase in the Pi treatment ($P < 0.0012$, Table S1, Figure S1).

3.2 Soil abiotic and biotic properties

Nitrogen inputs significantly increased soil DIN content ($P < 0.0001$) and decreased soil pH ($P = 0.0003$), MBC ($P = 0.0202$), fungal biomass ($P = 0.0253$), and exchangeable Mg^{2+} ($P = 0.0031$, Tables 1 and S2). Warming amplified the N effect on pH values (N×W, $P = 0.0478$, Table S2). Warming significantly increased root biomass ($P = 0.0145$) and soil DOC ($P = 0.0044$), but decreased fungal biomass ($P = 0.0244$, Tables 1 and S2, Figure 5a–c). Increased precipitation significantly increased soil fungal ($P = 0.0481$) and eukaryote biomass ($P = 0.0354$) and exchangeable Mg^{2+} ($P = 0.0072$, Tables 1, S2 and S4). Soil carbonate was marginally significantly affected by the interactive effect of precipitation alteration and N addition ($P = 0.0799$, Figure 2a

and Table S2). Without N inputs, increased precipitation significantly decreased the soil carbonate content by 10.4% (Pi treatments compared with Pr treatments). Without N inputs, exchangeable Mg^{2+} was significantly negative correlated with soil carbonate content (P = 0.0018, Figure 2b). However, the three factors and their interactions did not affect total SOC, biomass of Gram-positive bacteria, Gram-negative bacteria, actinomycetes and anaerobe, or exchangeable Ca^{2+} (Tables S2 and S4).

3.3 Soil aggregate size distribution, C content and soil respiration

Increased precipitation (without N inputs) significantly increased the mass proportion of macroaggregates and MWD. However, the promotional effect was attenuated by N inputs (N×P, P = 0.0469; P = 0.0583, Figure 3, Tables 2 and S3). Warming and N inputs had no effect on MWD (Table S3). Without N inputs, MWD was significantly related to soil exchangeable Mg^{2+} (P = 0.0090, Figure 4a) and fungal biomass (P = 0.0060, Figure 4b), while the positive relationships of MWD with both soil exchangeable Mg^{2+} and fungal biomass were decoupled with N inputs (Figure 4). However, we did not find a significant relationship between soil exchangeable Ca^{2+} and MWD (Figure S2). Warming significantly decreased soil respiration during the growing season in 2018 (P = 0.0010, Figure 5d). Also, warming significantly increased organic C content in silt-clay fractions by 4.1% (P = 0.0469, Figure 5e).

4. Discussion

4.1 Nitrogen inputs negated the positive effects of increased precipitation on soil aggregate stability

Our results showed that in the absence of N inputs, simulated increased precipitation significantly enhanced soil aggregation, as evidenced by mean weight diameter (MWD) (Figures 3, Table S3). This result is consistent with our hypothesis 1 and suggests that soil moisture may critically affect soil C persistence in water-limiting systems. Precipitation increase may affect soil aggregation via both geochemical and biological processes (Figure 6). Added precipitation directly increases soil moisture and the availability of cations in solution, which likely promote the formation of cation

bridging as positively charged cations function as the binding agent between negatively charged clay surfaces and organic compounds (Clarholm et al., 2015; Totsche et al., 2017). Alkaline soils on the Loess plateau are usually enriched with Ca and Mg carbonates (Chen, 2005). Precipitation increase could promote water diffusion, root and microbial activties and biological CO_2 production in soil microsites, which can accelerate the dissolution of calcium or magnesium carbonate ($CO_2 + H_2O + CaCO_3/MgCO_3 \rightarrow Ca^{2+}/Mg^{2+} + 2HCO_3^-$) (Emmerich, 2003). Also, because $MgCO_3$ ($Ksp = 3.5 \times 10^{-8}$) has a higher solubility than $CaCO_3$ ($Ksp = 2.9 \times 10^{-9}$), precipitation increase should promote more Mg^{2+} than Ca^{2+} release, as evidenced by the observed increase in Mg^{2+} and the decrease in carbonate content (Table 1, Figure 2). In the absence of N inputs, enhanced exchangeable Mg^{2+} as a result of precipitation increase (Tables 1 and S2) may have contributed to soil microaggregate formation by cation bridging (Bronick and Lal, 2005; Rowley et al., 2018), consistent with the observed MWD increase (Figures 3 and 4a). The lack of significant correlation between MWD and Ca^{2+} (Figure S2), the dominant polyvalent cation in this alkaline soil (Table 1), suggests that most of the Ca released by the ammonium acetate extraction may have been associated with carbonate, and thus was not directly bound with soil organic C.

Increased soil moisture may also enhance biological processes that promote aggregate formation. Significantly higher fungal biomass and its correlation with MWD under precipitation increase (Figure 4b, Table S2) suggest that fungal hyphae and their extracellular polymeric substances (EPS) may have significantly contributed to aggregate formation in our system (Figure 6) (Miller & Jastrow, 1990; Hu et al., 1995; Costa et al., 2018). Polysaccharides, chitins, and proteins can bind soil clays into microaggregates, and fungal hyphae often enmesh microaggregates into macroaggregates (Tisdall & Oades, 1982). Together, our results suggest that precipitation increase alone may stimulate both geochemical (e.g., Mg^{2+}-OC binding) and biological processes (e.g., fungal growth) to promote the formation and stability of soil aggregates in arid systems, possibly enhancing organic C persistence in soil.

Other factors, reactive N inputs in particular, may, however, interact with precipitation to influence the formation and stability of soil aggregates (Figure 6). Although N inputs did not significantly reduce soil aggregation across all treatments (Table S3), they did negate the positive

effects of increased precipitation on soil aggregation (Figure 3). Reactive N inputs often reduce soil pH because biological ammonium uptake is balanced by proton release, and because nitrification generates protons and nitrate. While nitrate and cations are prone to leaching with water, protons remain in soil and increase soil acidity (Barak et al., 1997; Bowman et al., 2008; Horswill et al., 2008). Free protons in soil solution may reduce the formation of clay-Mg^{2+}-OC complexes as H^+ may replace Mg^{2+} (Oades, 1988). Also, reactive N inputs often suppress the growth of both saprophytic fungi and arbuscular mycorrhizal fungi (AMF) (Treseder, 2004; Zhang et al., 2018), reducing extraradical hyphal density of AMF and altering the AMF community composition (van Diepen et al., 2011; Liu et al., 2012). A reduction in saprophytic fungal and AMF hyphae may suppress aggregate formation by reducing EPS binding of soil clays into microaggregate and hyphal enmeshment of microaggregates (Tisdall & Oades, 1982; Sheldrake et al., 2018). The decoupling between fungal PLFAs and MWD under N inputs observed in our study (Figure 4b) provided evidence suggesting that N-mediated suppression of fungi can cascade up to affect soil aggregation. Taken together, these results indicate that N inputs can significantly modify the effect of precipitation alteration on soil aggregation (Figure 6), suggesting that predictions based on single-factor experiments might be misleading.

4.2 Warming increased mineral-associated C content.

Contrary to our expectation that SOC would decrease under warming as a consequence of increased decomposition (Hypothesis 3), warming increased mineral-associated C content (Figure 5e). This may have resulted from increased labile C transformation into mineral-associated C. The observed increase in root biomass and DOC under the warming treatment (Figure 5a and b) provided a source of microbe- and/or plant-derived soluble organic compounds that could sorb or co-precipitate with soil minerals to increase mineral-associated C (Huang et al., 2019).

Another possible mechanism contributing to the increased mineral-associated C under warming was the suppressed decomposition of the existing mineral-associated C due to warming-induced water limitation and changes in the microbial community. Mineral-associated C has long been believed to be stable as it may be largely unavailable for microbial breakdown.

Increasing evidence has, however, shown that a couple mechanisms may promote the release of this C and make it available for microbes in a short time scale of days to months. For example, oxalic acid, a common component of root exudate, promotes C loss by liberating organic compounds from protective associations with minerals (Keiluweit et al., 2015). Also, high soil moisture within microsites induced by precipitation increase may promote iron (Fe) reduction that further releases protected C (Huang & Hall, 2017), as well as enhance activities of hydrolases (Henry et al., 2005). Lower soil respiration under warming observed in our study (Figure 5d) may have resulted from decreases in soil moisture due to higher evapotranspiration, as soil temperature at 10 cm depth was not affected (Figure S1, Table S1). Water limitation is often the primary factor regulating microbial decomposition in arid systems (Liu et al., 2009; Carbone et al., 2011), and the stimulation of root growth under warming (Figure 5a) may exacerbate water limitation. Increasing experimental evidence has shown that when water is not limiting, warming reduces SOC by enhancing degradation of older C via shifting the microbial functional community and enhancing catabolic potential (Zhang et al., 2005; Cheng et al., 2017; Feng et al., 2017). However, warming-induced decreases of soil fungal biomass (Figure 5c) may have suppressed fungal decomposition activities. Our field results suggest that in arid ecosystems, increased belowground plant biomass under warming, along with suppressed soil respiration due to warming-driven water limitation and suppression of fungal biomass, may lead to a possible increase in silt-clay C.

5. Conclusions and implications for soil C persistence and change in arid and semi-arid ecosystems

Understanding the interactive effects of multiple factors on soil C persistence is important for accurately predicting ecosystem C balances under future global change scenarios. Results from our field study showed that in the absence of N inputs, precipitation addition enhanced soil aggregation and promoted the coupling between aggregation and both soil fungal biomass and exchangeable Mg^{2+}. However, N inputs offset the promotional effects of increased precipitation, likely through suppressing fungal growth and altering soil pH and clay-Mg^{2+}-OC bridging (Figure 6). Also, warming increased mineral-associated C content, likely due to warming-enhancement of

labile C inputs and reduced turnover of existing mineral-associated C due to suppression of fungal growth and soil respiration. Together, these results suggest that results from single factor-manipulation experiments may have limited power to predict the C dynamics in the future. Given that grassland soils in semi-arid environments store large amounts of C in both organic and inorganic forms (Jobbagy & Jackson 2000; Lal, 2004), our findings highlight the importance of incorporating multi-factor interactive effects on soil C dynamics into models of water-limited ecosystems across the globe.

Acknowledgements

We thank the Ningxia Yunwu Mountain Preserve Administration for providing logistical support. This work was supported by National Key R&D Program of China (No. 2017YFC0503902) and National Natural Science Foundation of China (NSFC) (No. 41671269).

Data accessibility

The data that support the findings of this study are available from the authors upon reasonable request.

References

Ahlstrom, A., Raupach, M. R., Schurgers, G., Smith, B., Arneth, A., Jung, M., … Zeng, N. (2015). The dominant role of semi-arid ecosystems in the trend and variability of the land CO_2 sink. *Science, 348*, 895–899.

Amundson, R. G., Trask, J., & Pendall, E. (1988). A rapid method of soil carbonate analysis using gas chromatography. *Soil Science Society of America Journal, 52*, 880–883.

Barak, P., Jobe, B. O., Krueger, A. R., Peterson, L. A., & Laird, D. A. (1997). Effects of long-term soil acidification due to nitrogen fertilizer inputs in wisconsin. *Plant & Soil, 197*, 61–69.

Berhe, A. A., Suttle, K. B., Sarah D. B., & Banfield, J. F. (2012). Contingency in the direction and mechanics of soil organic matter responses to increased rainfall. *Plant & Soil, 358*, 371–383.

Bossio, D. A., & Scow, K. M. (1998). Impacts of carbon and flooding on soil microbial communities:

phospholipid fatty acid profiles and substrate utilization patterns. *Microbial Ecology, 35*, 265–278.

Bowman, W. D., Cleveland, C. C., Halada, L., Hresko, J., & Baron, J. S. (2008). Negative impact of nitrogen deposition on soil buffering capacity. *Nature Geoscience, 1*, 767–770.

Bronick, C. J., & Lal, R. (2005). Soil structure and management: a review. *Geoderma, 124*, 3–22.

Campos, X., Germino, M., & de Graaff, M. A. (2017). Enhanced precipitation promotes decomposition and soil C stabilization in semiarid ecosystems, but seasonal timing of wetting matters. *Plant & Soil, 416*, 427–436.

Carbone, M. S., Still, C. J., Ambrose, A. R., Dawson, T. E., Williams, A. P., Boot, C. M., … Schimel, J. P. (2011). Seasonal and episodic moisture controls on plant and microbial contributions to soil respiration. *Oecologia, 167*, 265–278.

Castro Filho, C., Lourenco, A., Guimaraes, M. d. F., Fonseca, I. C. B. (2002). Aggregate stability under different soil management systems in a red latosol in the state of Parana, Brazilia. *Soil & Tillage Research, 65*, 45–51.

Chen, D., Li, J. J., Lan, Z. C., Hu, S. J., & Bai, Y. F. (2016). Soil acidification exerts a greater control on soil respiration than soil nitrogen availability in grasslands subjected to long-term nitrogen enrichment. *Functional Ecology, 30*, 658–669.

Chen, X. L. (2005). Change of late cenozoic climate and source regions recorded by carbonates on Chinese central Loess Plateau (Doctoral dissertation). Lanzhou University.

Chen, Z. M., Xu, Y. H., Zhou, X. H., Tang, J. W., Kuzyakov, Y., Yu, H. Y., … Ding, W. X. (2017). Extreme rainfall and snowfall alter responses of soil respiration to nitrogen fertilization: a 3-year field experiment. *Global Change Biology, 23*, 3403–3417.

Cheng, L., Zhang, N. F., Yuan, M. T., Xiao, J., Qin, Y. J., Deng, Y., … Zhou, J. Z. (2017). Warming enhances old organic carbon decomposition through altering functional microbial communities. *The ISME Journal, 11*, 1825–1835.

Clarholm, M., Skyllberg, U., & Rosling, A. (2015). Organic acid induced release of nutrients from metal-stabilized soil organic matter - the unbutton model. *Soil Biology & Biochemistry, 84*, 168–176.

Costa, O. Y. A., Raaijmakers, J. M., & Kuramae, E. E. (2018). Microbial extracellular polymeric substances: ecological function and impact on soil aggregation. *Frontiers in Microbiology, 9*, 1636.

Dietzen, C. A., Larsen, K. S., Ambus, P. L., Michelsen, A., Arndal, M. F., Beier, C., … Schmidt, I. K. (2019).

Accumulation of soil carbon under elevated CO_2 unaffected by warming and drought. *Global Change Biology, 25*, 2970–2977.

Dillon, M. E., Wang, G., & Huey, R. B. (2010). Global metabolic impacts of recent climate warming. *Nature, 467*, 704–706.

Dungait, J. A. J., Hopkins, D. W., Gregory, A. S., & Whitmore, A. P. (2012). Soil organic matter turnover is governed by accessibility not recalcitrance. *Global Change Biology, 18*, 1781–1796.

Emmerich, W. E. (2003). Carbon dioxide fluxes in a semiarid environment with high carbonate soils. *Agricultural Forest & Meteorology, 116*, 91–102.

Feng, W. T., Liang, J. Y., Hale, L. E., Jung, C. G., Chen, J., Zhou, J. Z., … Luo, Y. Q. (2017). Enhanced decomposition of stable soil organic carbon and microbial catabolic potentials by long-term field warming. *Global Change Biology, 23*, 4765–4776.

Griepentrog, M., Bode, S., Boeckx, P., Hagedorn, F., Heim, A., & Schmidt, M. W. I. (2014). Nitrogen deposition promotes the production of new fungal residues but retards the decomposition of old residues in forest soil fractions. *Global Change Biology, 20*, 327–340.

Guan, S., An, N., Zong, N., He, Y. T., Shi, P. L., Zhang, J. J., & He, N. P. (2018). Climate warming impacts on soil organic carbon fractions and aggregate stability in a Tibetan alpine meadow. *Soil Biology & Biochemistry, 116*, 224–236.

Guo, L., Cheng, J., Luedeling, E., Koerner, S. E., He, J. S., Xu, J. C., … Peng, C. H. (2017). Critical climate periods for grassland productivity on China's Loess Plateau. *Agricultural & Forest Meteorology, 233*, 101–109.

Hendershot, W. H, Lalande, H. & Duquette, M. (1993). in *Soil Sampling and Methods of Analysis* (ed. Carter, M. R.) (pp. 167–176). Lewis Publishers, Boca Raton.

Henry, H. A. L., Juarez, J. D., Field, C. B., & Vitousek, P. M. (2005). Interactive effects of elevated CO_2, N deposition and climate change on extracellular enzyme activity and soil density fractionation in a Californian annual grassland. *Global Change Biology, 11*, 1808–1815.

Horswill, P., O'Sullivan, O., Phoenix, G. K., Lee, J. A., & Leake, J. R. (2008). Base cation depletion, eutrophication and acidification of species-rich grasslands in response to long-term simulated nitrogen deposition. *Environmental Pollution, 155*, 336–349.

Hu, S., Coleman, D. C., Beare, M. H., & Hendrix, P. F. (1995). Soil carbohydrates in aggrading and degrading agroecosystems: influences of fungi and aggregates. *Agriculture Ecosystems & Environment, 54*, 77–88.

Huang, W. J., & Hall, S. J. (2017). Elevated moisture stimulates carbon loss from mineral soils by releasing protected organic matter. *Nature Communications, 8*, 1774.

Huang, W. J., Hammel, K. E., Hao, J. L., Thompson, A., Timokhin, V. I., & Hall, S. J. (2019). Enrichment of lignin-derived carbon in mineral-associated soil organic matter. *Environmental Science & Technology, 53*, 7522–7531.

IPCC. (2013). *Climate Change 2013 – The Physical Science Basis: Working Group I Contribution to the Fifth Assessment Report of the Intergovernmental Panel on Climate Change.* Cambridge University Press, Cambridge.

Jobbagy, E. E. G., & Jackson, R. B. (2000). The vertical distribution of soil organic carbon and its relation to climate and vegetation. *Ecological Applications, 10*, 423–436.

Keiluweit, M., Bougoure, J. J., Nico, P. S., Pett-Ridge, J., Weber, P. K., & Kleber, M. (2015). Mineral protection of soil carbon counteracted by root exudates. *Nature Climate Change, 5*, 588–595.

Lal, R. (2004). Soil carbon sequestration impacts on global climate change and food security. *Science, 304*, 1623–1627.

Lal, R. (2008). Carbon sequestration. *Philosophical Transactions of the Royal Society B: Biological Sciences, 363*, 815–830.

Lehmann, A., Zheng, W. S., & Rillig, M. C. (2017). Soil biota contributions to soil aggregation. *Nature Ecology & Evolution, 1*, 1828–1835.

Lehmann, J., & Kleber, M. (2015). The contentious nature of soil organic matter. *Nature, 528*, 60–68.

Liu, L. L., Wang, X., Lajeunesse, M. J., Miao, G. F., Piao, S. L., Wan, S. Q., … Deng, M. F. (2016). A cross-biome synthesis of soil respiration and its determinants under simulated precipitation changes. *Global Change Biology, 22*, 1394–1405.

Liu, W. X., Zhang, Z., & Wan, S. Q. (2009). Predominant role of water in regulating soil and microbial respiration and their responses to climate change in a semiarid grassland. *Global Change Biology, 15*, 184–195.

Liu, Y. J., Shi, G. X., Mao, L., Cheng, G., Jiang, S. J., Ma, X. J., … Feng, H. Y. (2012). Direct and indirect

influences of 8 yr of nitrogen and phosphorus fertilization on Glomeromycota in an alpine meadow ecosystem. *New Phytologist, 194*, 523–535.

Lu, M., Zhou, X. H., Luo, Y. Q., Yang, Y. H., Fang, C. M., Chen, J. K., & Li, B. (2011). Minor stimulation of soil carbon storage by nitrogen addition: A meta-analysis. *Agriculture, Ecosystem & Environent, 140*, 234–244.

Miller, R. M., & Jastrow, J. D. (1990). Hierarchy of root and mycorrhizal fungal interactions with soil aggregation. *Soil Biology & Biochemistry, 22*, 579–584.

Ni, X. Y., Yang, W. Q., Qi, Z. M., Liao, S., Xu, Z. F., Tan, B., … Wu, F. Z. (2017). Simple additive simulation overestimates real influence: altered nitrogen and rainfall modulate the effect of warming on soil carbon fluxes. *Global Change Biology, 23*, 3371–3381.

Oades, J. M. (1988). The retention of organic matter in soils. *Biogeochemistry, 5*, 35–70.

Poeplau, C., Katterer, T., Leblans, N. I. W., & Sigurdsson, B. D. (2017). Sensitivity of soil carbon fractions and their specific stabilisation mechanisms to extreme soil warming in a subarctic grassland. *Global Change Biology, 23*, 1316–1327.

Poulter, B., Frank, D., Ciais, P., Myneni, R. B., Andela, N., Bi, J., … van der Werf, G. R. (2014). Contribution of semi-arid ecosystems to interannual variability of the global carbon cycle. *Nature, 509*, 600–603.

Quinn, G. P., & Keough, M. J. (2002). *Experimental Design and Data Analysis for Biologists*. Cambridge, England: Cambridge University Press.

Rillig, M. C., Wright, S. F., Shaw, M. R., & Field, C. B. (2002). Artificial climate warming positively affects arbuscular mycorrhizae but decreases soil aggregate water stability in an annual grassland. *Oikos, 97*, 52–58.

Rillig, M. C., Ryo. M., Lehmann. A., Aguilar-Trigueros, C. A., Buchert, S., Wulf, A., … Yang, G. W. (2019). The role of multiple global change factors in driving soil functions and microbial biodiversity. *Science, 366*, 886–890.

Rowley, M. C., Grand, S., & Verrecchia, E. P. (2018). Calcium-mediated stabilisation of soil organic carbon. *Biogeochemistry, 137*, 27–49.

Schmidt, M. W. I., Torn, M. S., Abiven, S., Dittmar, T., Guggenberger, G., Janssens, I. A., … Trumbore, S. E. (2011). Persistence of soil organic matter as an ecosystem property. *Nature, 478*, 49–56.

Sheldrake, M., Rosenstock, N. P., Mangan, S., Revillini, D., Sayer, E. J., Ollson, P. A., … Wright, S. J. (2018). Responses of arbuscular mycorrhizal fungi to long-term inorganic and organic nutrient addition in a lowland tropical forest. *The ISME Journal, 12*, 2433–2445.

Shen, D. Y., Ye, C. L., Hu, Z. K., Chen, X. Y., Guo, H., Li, J. Y., … Liu, M. Q. (2018). Increased chemical stability but decreased physical protection of soil organic carbon in response to nutrient amendment in a Tibetan alpine meadow. *Soil Biology & Biochemistry, 126*, 11–21.

Six, J., Bossuyt, H., Degryze, S., & Denef, K. (2004). A history of research on the link between (micro)aggregates, soil biota, and soil organic matter dynamics. *Soil & Tillage Research, 79*, 7–31.

Stewart, C. E., Plante, A. F., Paustian, K., Conant, R. T., & Six, J. (2008). Soil carbon saturation: linking concept and measurable carbon pools. *Soil Science Society of America Journal, 72*, 379–392.

Tamura, M., Suseela, V., Simpson, M., Powell, B., & Tharayil, N. (2017). Plant litter chemistry alters the content and composition of organic carbon associated with soil mineral and aggregate fractions in invaded ecosystems. *Global Change Biology, 23*, 4002–4018.

Tisdall, J. M., & Oades, J. M. (1982). Organic matter and water-stable aggregates in soils. *Journal of Soil Science, 33*, 141–163.

Totsche, K. U., Amelung, W., Gerzabek, M. H., Guggenberger, G., Klumpp, E., Knief, C., … Kogel-Knabner, I. (2017). Microaggregates in soils. *Journal of Plant Nutrition and Soil Science, 181*, 104–136.

Treseder, T. T. (2004). A meta-analysis of mycorrhizal responses to nitrogen, phosphorus, and atmospheric CO_2 in field studies. *New Phytologist, 164*, 347–355.

Vance, E. D., Brookes, P. C., & Jenkinson, D. S. (1987). An extraction method for measuring soil microbial biomass C. *Soil Biology & Biochemistry, 19*, 703–707.

van Diepen, L. T. A., Lilleskov, E. A., & Pregitzer, K. S. (2011). Simulated nitrogen deposition affects community structure of arbuscular mycorrhizal fungi in northern hardwood forests. *Molecular Ecology, 20*, 799–811.

Wan, S., Norby, R. J., Ledford, J., & Weltzin, J. F. (2007). Responses of soil respiration to elevated CO_2, air warming, and changing soil water availability in a model old-field grassland. *Global Change Biology, 13*, 2411–2424.

Wang, N., Quesada, B., Xia, L. L., Butterbach-Bahl, K., Goodale, C. L., & Kiese, R. (2019). Effects of climate

warming on carbon fluxes in grasslands–A global meta-analysis. *Global Change Biology, 25*, 1839–1851.

Wilson, G. W. T., Rice, C. W., Rillig, M. C., Springer, A., & Hartnett, D. C. (2009). Soil aggregation and carbon sequestration are tightly correlated with the abundance of arbuscular mycorrhizal fungi: results from long-term field experiments. *Ecology Letters, 12*, 452–461.

Wu, H. B., Guo, Z. T., Gao, Q., & Peng, C. H. (2009). Distribution of soil inorganic carbon storage and its changes due to agricultural land use activity in China. *Agriculture Ecosystems & Environment, 129*, 413–421.

Ye, C. L., Chen, D. M., Hall, S. J., Pan, S., Yan, X. B., Bai, T. S., … Hu, S. J. (2018). Reconciling multiple impacts of nitrogen enrichment on soil carbon: plant, microbial and geochemical controls. *Ecology Letters, 21*, 1162–1173.

Yu, G. H., Xiao, J., Hu, S. J., Polizzotto, M. L., Zhao, F. J., Mcgrath, S. P., … Shen, Q. R. (2017). Mineral availability as a key regulator of soil carbon storage. *Environmental Science & Technology, 51*, 4960–4969.

Yue, K., Fornara, D. A., Yang, W. Q., Peng, Y., Peng, C. H., Liu, Z, L., & Wu, F. Z. (2017). Influence of multiple global change drivers on terrestrial carbon storage: additive effects are common. *Ecology Letters, 20*, 663–672.

Zamanian, K., Zarebanadkouki, M., & Kuzyakov, Y. (2018). Nitrogen fertilization raises CO_2 efflux from inorganic carbon: A global assessment. *Global Change Biology, 24*, 2810–2817.

Zhang, T. A., Chen, H. Y. H., & Ruan, H. H. (2018). Global negative effects of nitrogen deposition on soil microbes. *The ISME Journal, 12*, 1817–1825.

Zhang, W., Parker, K. M., Luo, Y., Wan, S., Wallace, L. L., & Hu, S. (2005). Soil microbial responses to experimental warming and clipping in a tallgrass prairie. *Global Change Biology, 11*, 266–277.

Zhou, L. Y., Zhou, X. H., Shao, J. J., Nie, Y. Y., He, Y. H., Jiang, L. L., … Bai, S. H. (2016). Interactive effects of global change factors on soil respiration and its components: a meta-analysis. *Global Change Biology, 22*, 3157–3169.

Zhou, X. Q., Chen, C. R., Wang, Y. F., Xu, Z. H., Hu, Z. Y., Cui, X. Y., & Hao, Y. B. (2012). Effects of warming and increased precipitation on soil carbon mineralization in an Inner Mongolian grassland after 6 years of treatments. *Biology & Fertility of Soils, 48*, 859–866.

Table 1 Effects of warming, N inputs, and altered precipitation on soil abiotic and biotic properties. Data are means and standard errors (n = 4).

	SOC (mg kg^{-1} soil)	Carbonate (mg kg^{-1} soil)	pH	Root biomass (g kg^{-1} soil)	DIN (mg kg^{-1} soil)	DOC (mg kg^{-1} soil)	MBC (mg kg^{-1} soil)	Fungi PLFA (nmol g^{-1} soil)	Bacteria PLFA (nmol g^{-1} soil)	Exchangeable Ca^{2+} (mg kg^{-1} soil)	Exchangeable Mg^{2+} (mg kg^{-1} soil)	Soil respiration (μmol m^2 s^{-1})
CK	37.15 (1.75)	5.57 (0.32)	7.78 (0.06)	5.85 (0.61)	9.81 (0.80)	171.1 (10.1)	746.6 (43.8)	16.92 (0.88)	102.0 (1.3)	7418 (630)	211.7 (4.9)	5.09 (0.69)
N	37.56 (0.64)	5.15 (0.26)	7.75 (0.05)	5.19 (0.46)	17.28 (1.90)	188.6 (10.2)	754.6 (39.3)	16.73 (1.70)	108.0 (8.5)	7182 (635)	201.3 (6.7)	5.33 (0.43)
W	38.35 (1.53)	5.06 (0.42)	7.83 (0.04)	6.40 (0.36)	11.13 (0.56)	226.6 (11.7)	901.2 (38.3)	16.50 (0.41)	103.5 (5.4)	7027 (827)	229.7 (10.3)	4.75 (0.52)
NW	37.73 (0.91)	4.89 (0.22)	7.72 (0.08)	6.74 (0.53)	25.18 (7.98)	227.9 (24.3)	668.8 (59.7)	14.87 (0.69)	100.8 (6.9)	6930 (719)	214.3 (14.5)	3.95 (0.32)
Pr	36.75 (1.16)	5.61 (0.15)	7.85 (0.04)	3.99 (0.46)	10.79 (0.69)	177.8 (6.8)	804.8 (33.7)	16.54 (0.41)	107.0 (2.9)	8211 (604)	225.1 (8.4)	4.65 (0.58)
NPr	36.52 (0.68)	5.00 (0.18)	7.77 (0.05)	4.96 (0.74)	13.63 (0.99)	184.0 (4.1)	782.2 (54.7)	15.90 (1.06)	106.3 (3.8)	7633 (737)	202.0 (8.4)	4.55 (0.49)
WPr	36.57 (2.35)	5.55 (0.24)	7.86 (0.04)	6.21 (2.66)	8.90 (0.23)	206.9 (33.8)	810.2 (56.1)	15.40 (1.19)	100.7 (2.6)	7674 (708)	210.8 (7.6)	4.47 (0.30)
NWPr	38.31 (0.39)	4.76 (0.24)	7.65 (0.11)	6.71 (0.36)	22.18 (6.71)	225.1 (17.6)	821.1 (38.4)	12.84 (1.58)	92.3 (10.3)	6998 (399)	208.4 (4.0)	3.82 (0.17)
Pi	39.77 (0.78)	4.93 (0.16)	7.79 (0.07)	5.55 (0.73)	10.74 (1.03)	179.0 (2.5)	875.8 (57.9)	19.00 (0.64)	114.8 (5.6)	7669 (767)	250.8 (10.7)	5.66 (0.72)
NPi	35.82 (1.75)	5.25 (0.43)	7.72 (0.05)	5.81 (1.89)	14.97 (1.69)	173.6 (22.3)	763.6 (50.9)	15.74 (1.03)	107.3 (6.6)	6594 (560)	209.6 (7.5)	5.83 (0.86)
WPi	36.43 (1.00)	5.08 (0.27)	7.93 (0.04)	6.11 (1.10)	10.42 (0.75)	163.5 (9.9)	845.5 (51.1)	16.45 (1.17)	104.1 (7.1)	7878 (858)	232.6 (10.1)	4.83 (0.22)
NWPi	38.30 (0.58)	4.94 (0.17)	7.73 (0.06)	9.46 (1.46)	16.77 (1.39)	195.3 (11.0)	834.8 (30.3)	16.68 (0.85)	113.4 (5.4)	7504 (676)	229.7 (11.5)	4.05 (0.19)
Significance ($P < 0.05$)	n.s.	N	N N×W	W	N	W	N N×W×P	N W P	n.s.	n.s.	N P	W

CK: Control; N: Nitrogen inputs; W: Warming; NW: Nitrogen inputs + Warming; Pr: Precipitation reduction; NPr: Nitrogen inputs + Precipitation reduction; WPr: Warming + Precipitation reduction; NWPr: Nitrogen inputs + Warming + Precipitation reduction; Pi: Precipitation increase; NPi: Nitrogen inputs + Precipitation increase; WPi: Warming + Precipitation increase; NWPi: Nitrogen inputs + Warming + Precipitation increase.

SOC: soil organic C; DIN: dissolved inorganic N; DOC: dissolved organic C; MBC: microbial biomass C.

Table 2 Effects of warming, N input, and altered precipitation on mass distribution, C concentrations and C content in light fraction, macroaggregate, microaggregate and silt- and clay-C fractions. Data are means and standard errors (n = 4).

	Weight of light fraction (%)	Light fraction C concentration (mg kg^{-1} light fraction)	Light fraction C content (mg kg^{-1} soil)	Weight of macroaggregate fraction (%)	Macroaggregate C concentration (mg kg^{-1} Macroaggregate)	Macroaggregate C content (mg kg^{-1} soil)	Weight of microaggregate fraction (%)	Microaggregate C concentration (mg kg^{-1} Microaggregate)	Microaggregate C content (mg kg^{-1} soil)	Weight of silt-clay fraction (%)	Silt-clay C concentration (mg kg^{-1} silt-clay fraction)	Silt-clay C content (mg kg^{-1} soil)
CK	2.79 (0.23)	223.75 (6.96)	6.25 (0.60)	18.18 (1.56)	37.58 (2.15)	6.78 (0.54)	34.98 (1.01)	42.90 (1.67)	15.05 (0.96)	44.05 (1.99)	20.63 (0.61)	9.06 (0.35)
N	2.93 (0.39)	218.55 (3.98)	6.40 (0.85)	17.39 (0.72)	38.25 (2.00)	6.63 (0.32)	36.82 (0.31)	42.73 (1.17)	15.74 (0.55)	42.85 (0.55)	20.50 (0.32)	8.79 (0.20)
W	2.73 (0.17)	224.95 (7.46)	6.11 (0.23)	18.01 (1.28)	38.60 (1.75)	6.93 (0.50)	35.59 (1.41)	44.95 (2.09)	16.02 (1.09)	43.67 (0.82)	21.30 (0.42)	9.30 (0.16)
NW	3.06 (0.23)	219.23 (11.05)	6.65 (0.35)	20.52 (2.48)	37.25 (1.66)	7.53 (0.61)	32.89 (1.52)	43.83 (1.57)	14.42 (0.91)	43.53 (1.61)	20.95 (0.41)	9.13 (0.44)
Pr	2.19 (0.14)	224.73 (7.71)	4.95 (0.47)	17.80 (1.53)	38.20 (0.96)	6.81 (0.65)	36.03 (1.23)	43.35 (1.67)	15.60 (0.64)	43.97 (1.09)	21.38 (0.44)	9.39 (0.10)
NPr	2.87 (0.31)	219.70 (3.21)	6.32 (0.74)	17.65 (1.06)	36.55 (0.87)	6.46 (0.44)	33.56 (1.68)	42.50 (0.85)	14.23 (0.53)	45.91 (1.43)	20.73 (0.39)	9.51 (0.24)
WPr	2.50 (0.59)	223.08 (5.01)	5.64 (1.41)	17.93 (0.35)	37.50 (1.39)	6.72 (0.28)	32.83 (1.39)	43.15 (1.98)	14.18 (0.93)	46.74 (1.43)	21.48 (0.48)	10.03 (0.30)
NWPr	2.90 (0.15)	213.53 (7.42)	6.16 (0.17)	18.78 (2.14)	38.98 (1.58)	7.26 (0.66)	32.82 (2.61)	45.85 (1.20)	14.96 (0.92)	45.51 (0.82)	21.83 (0.47)	9.93 (0.24)
Pi	2.74 (0.36)	223.38 (10.17)	6.05 (0.65)	24.06 (1.35)	40.98 (1.19)	9.85 (0.58)	32.71 (0.71)	46.45 (0.89)	15.20 (0.50)	40.49 (0.45)	21.40 (0.49)	8.67 (0.26)
NPi	2.52 (0.45)	217.88 (0.19)	5.50 (0.98)	19.96 (0.59)	36.38 (1.24)	7.27 (0.37)	34.20 (2.13)	41.88 (1.63)	14.30 (0.97)	43.32 (1.89)	20.15 (0.61)	8.75 (0.61)
WPi	2.80 (0.34)	214.45 (8.28)	6.01 (0.79)	20.62 (0.92)	37.08 (1.21)	7.65 (0.45)	34.43 (1.28)	41.08 (0.66)	14.14 (0.54)	42.15 (0.78)	20.48 (0.23)	8.63 (0.22)
NWPi	3.23 (0.12)	215.08 (5.04)	6.96 (0.40)	17.65 (1.48)	36.70 (0.91)	6.45 (0.43)	35.01 (1.23)	44.45 (0.79)	15.54 (0.42)	44.10 (1.05)	21.18 (0.23)	9.34 (0.27)
Significant ($P < 0.05$)	n.s.	n.s.	n.s	P N×P	n.s.	P N×P W×P	n.s.	N×W	N×W×P	P	n.s.	W P

CK: Control; N: Nitrogen inputs; W: Warming; NW: Nitrogen inputs + Warming; Pr: Precipitation reduction; NPr: Nitrogen inputs + Precipitation reduction; WPr: Warming + Precipitation reduction; NWPr: Nitrogen inputs + Warming + Precipitation reduction; Pi: Precipitation increase; NPi: Nitrogen inputs + Precipitation increase; WPi: Warming + Precipitation increase; NWPi: Nitrogen inputs + Warming + Precipitation increase.

Figure 1 A partial overview of field experimental plots (a), open top chamber (OTC) for field warming (b) and the appliance used to decrease precipitation (c).

Figure 2 Effects of warming, N inputs, and altered precipitation on soil carbonate content (a) and relationship between soil carbonate and exchangeable Mg^{2+} (b). For simplification, the non-significant treatments are combined and only significant ($P < 0.05$) or marginally significant ($P < 0.1$) treatments and interactions are shown. Different letters indicate significant ($P < 0.05$) differences between altered precipitation treatments after simple main effects tests (n = 8).

Figure 3 Effects of warming, N inputs, and altered precipitation on mean weight diameter (MWD). For simplification, the non-significant treatments are combined and only significant ($P < 0.05$) or marginally significant ($P < 0.1$) treatments and interactions are shown. Different letters indicate significant ($P < 0.05$) differences between altered precipitation treatments after simple main effects tests (n = 8).

Figure 4 Relationships among mean weight diameter (MWD), soil exchangeable Mg^{2+} (a), and fungal phospholipid fatty acid (PLFA) (b) as influenced by N inputs.

Figure 5 Effects of warming on root biomass (a), dissolved organic C (DOC) (b), soil fungal PLFA (c), soil respiration (d) and silt-clay C content (e) (n = 24).

Figure 6 Contrasting effects of precipitation increase and N inputs on soil aggregation. While precipitation increase promotes soil aggregation through increasing soil exchangeable Mg^{2+} (geochemical process) and promoting fungal growth (biological process), reactive N input reduces soil aggregation through increasing soil N and proton (H^+) via nitrification and reducing fungal growth and metal-organic bridging. Black arrows refer to positive effects, and red arrows refer to negative effects

Figure 1

Figure 2

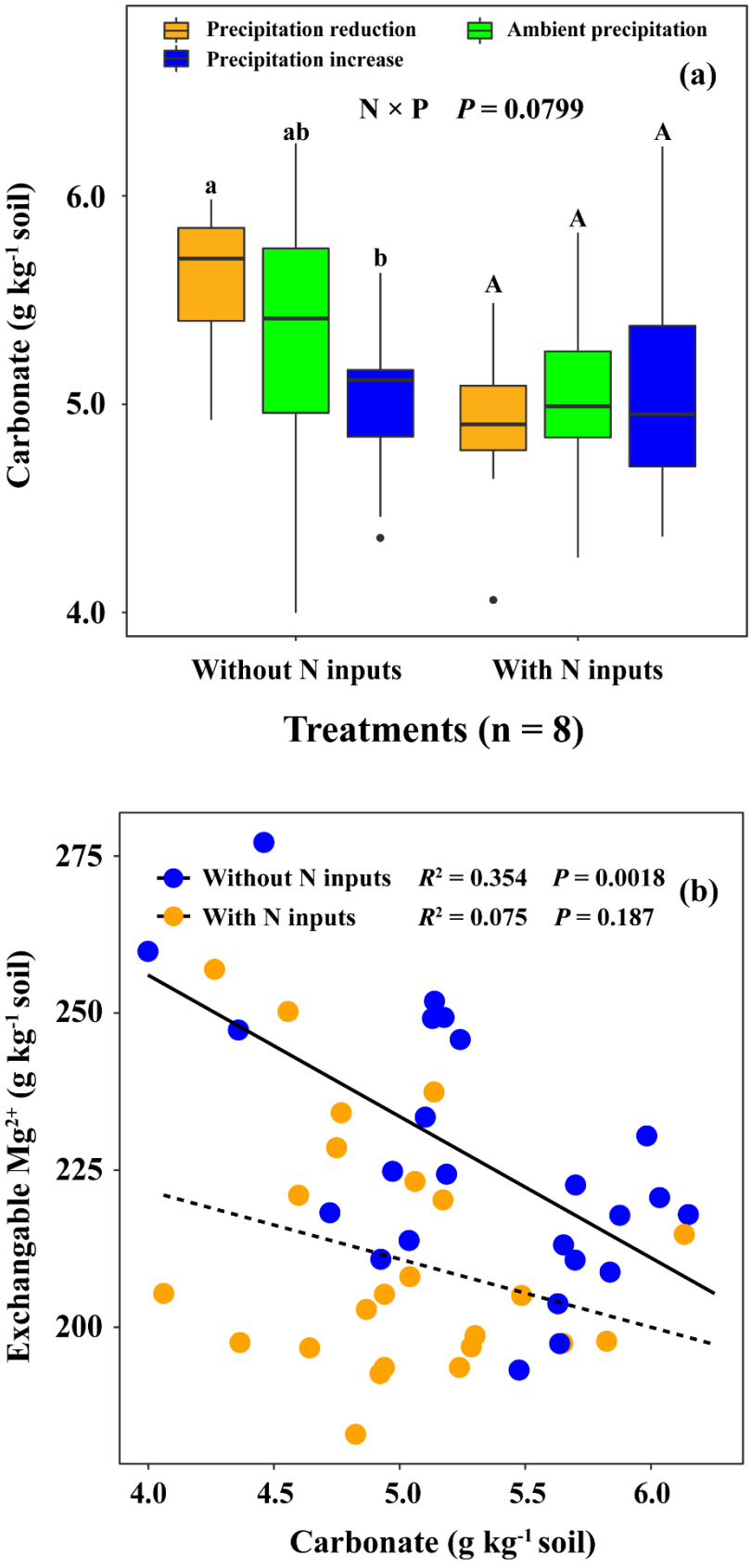

Figure 3

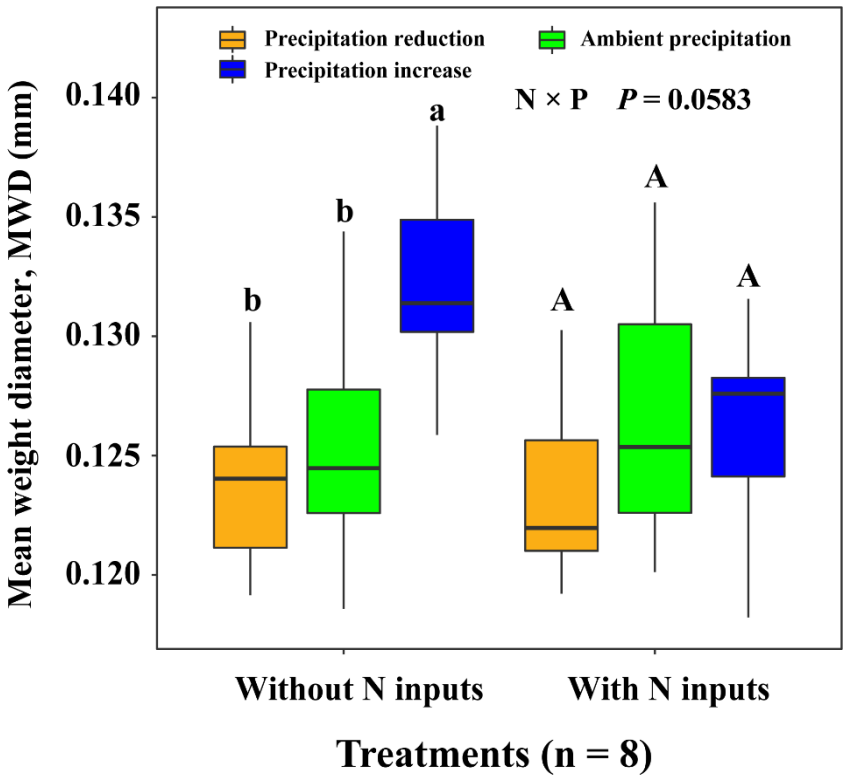

Figure 4

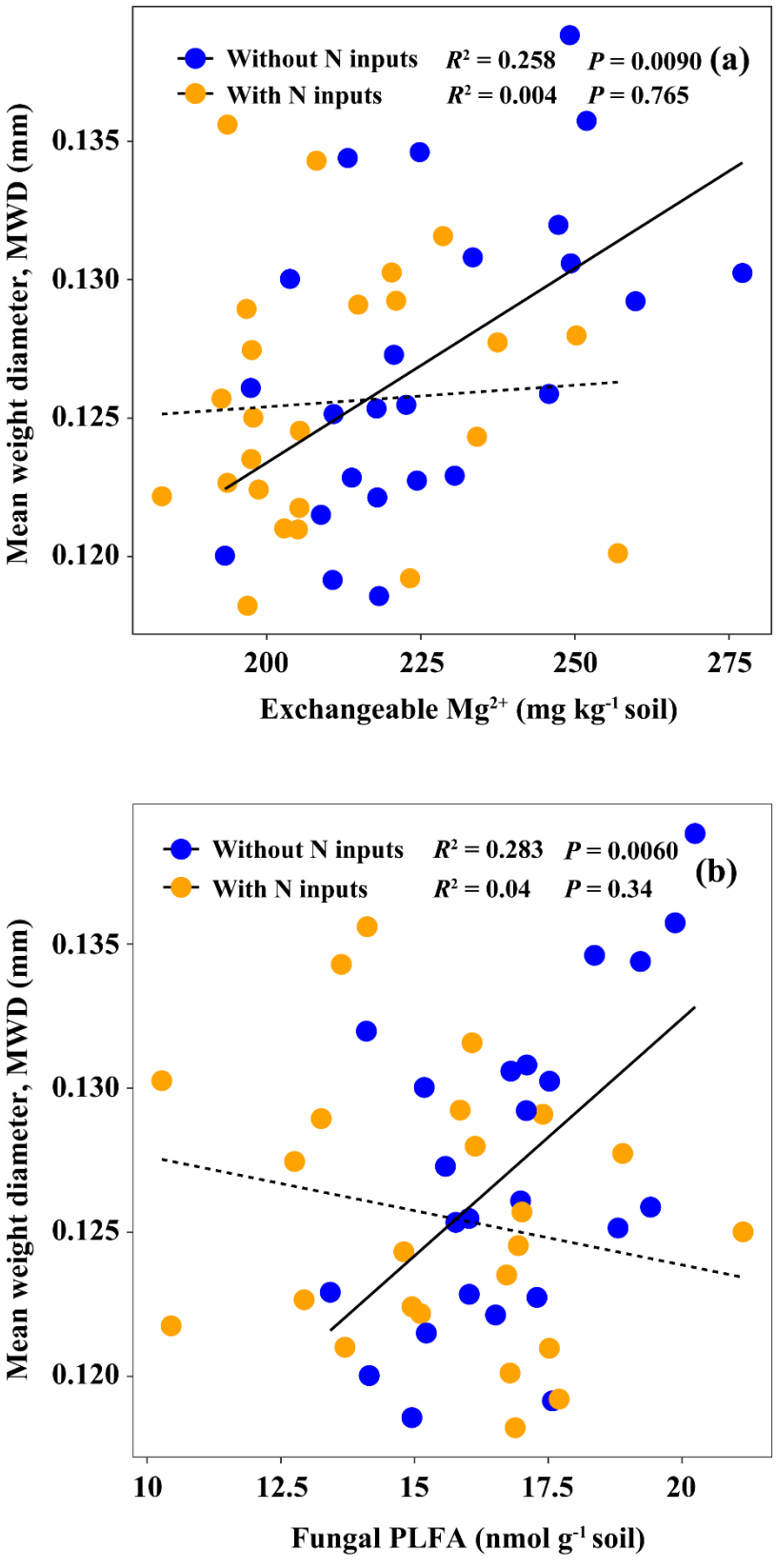

Figure 5

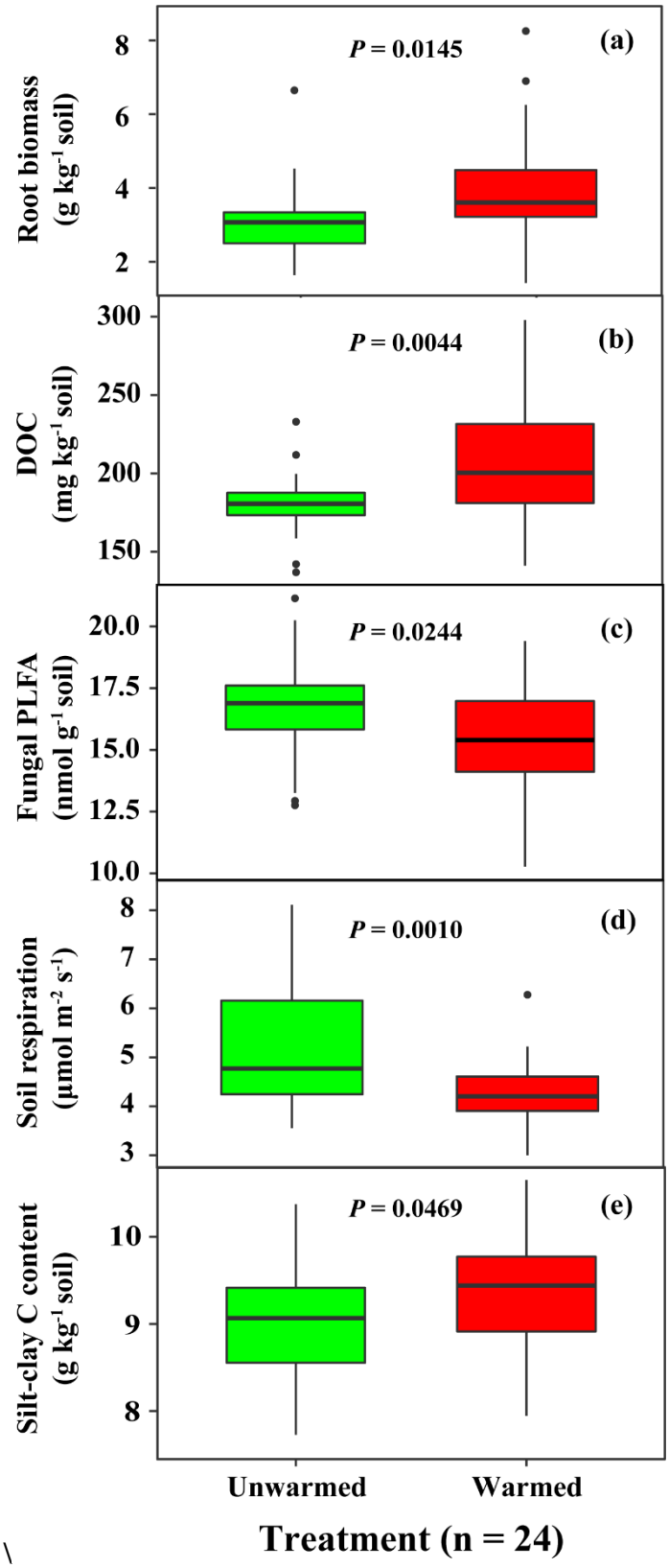

Figure 6